

ASTRO3DO

A THESIS SUBMITTED TO THE GRADUATE DIVISION OF THE
UNIVERSITY OF HAWAII AT MĀNOA IN PARTIAL FULFILLMENT
OF THE REQUIREMENTS FOR THE DEGREE OF

MASTER OF SCIENCE

IN

COMPUTER SCIENCE

MAY 2020

By

Michael J. Omori

Thesis Committee:

Peter Sadowski, Chairperson

John Shepherd

Kyungim Baek

Dan Suthers

Keywords: theses, dissertations, graduating, computer science, body composition, machine
learning

Copyright © 2020 by
Michael J. Omori

To those in need,
Those with or destined for cancer,
and the group.

ACKNOWLEDGMENTS

I want to thank god for this.

ABSTRACT

There are several key components of health, which can be monitored through means of body composition and shape analysis. Metrics such as fat mass index and fat free mass index are simple features of the human body that can aid our understanding in their overall health. How these are measured have been extensively studied throughout the years. Means such as DXA and bioimpedance can accurately measure body fat. While more recently, 3d imaging has proven to be able to match the performance of its predecessors whilst providing certain benefits such as lower cost. The Shepherd Lab has demonstrated such findings by showing similar results between DXA and 3d imaging. The project is ongoing and this thesis is the culmination of about 6 months relating to 3d imaging methods and testing for applications in space. It provides an overview of my work and the starting point of much future effort.

TABLE OF CONTENTS

Acknowledgments	iv
Abstract	v
List of Tables	vii
List of Figures	viii
1 Introduction	1
2 Previous Work	2
2.1 3d optical scanners	2
2.2 depth imaging	3
3 Methods	7
3.1 Graph Neural Network	7
3.2 Sensor Comparison	8
3.3 Categorical Extreme Gradient Boosting	9
3.4 Parabolic Flight Setup	9
3.5 Creating the ideal imaging setup on plane vs on ground	9
3.6 body imaging on babies	9
3.7 3d mesh modeling of humans	10
3.8 microgravity simulation	10
4 Results	11
4.1 sensor testing results	11
4.2 automated anthropometry results	13
4.3 gradient boosting body composition results	13
4.4 graph neural network body composition results	13
4.5 3d imaging testing results	13
5 Conclusion	15
5.1 Widgets	15
5.1.1 Sub-Widgets	15
A Some Ancillary Stuff	18
B More Ancillary Stuff	19
Bibliography	20

LIST OF TABLES

1.1	A normal size table.	1
-----	------------------------------	---

LIST OF FIGURES

2.1	Fit3d scanner	2
2.2	Naked Labs Scanner	4
2.3	Styku scanner	5
2.4	Sizestream scanner	6
4.1	Spatial resolution per frame of d435	11
4.2	Sensor accuracy by distance	12
4.3	Sensor temporal noise by distance	13
4.4	Fill rate of sensor by distance	14

CHAPTER 1

INTRODUCTION

Dual-energy x-ray absorptiometry (DXA) is commonly used to measure bone density by measuring the absorption of soft tissue and bone using dual x rays [1]. The radiation used is considered lower than normal; however, they should still be minimized in their usage which is why one would not want to take these every single day for example both for the health impacts and costs. Due to its versatility, DXA can also be used for total body composition and fat content measurement.

Body composition comprises of fat, bone, water, and muscle percentage. In what is known as the four compartment model [6]:

$$\frac{1}{D_b} = \frac{w}{D_w} + \frac{f}{D_f} + \frac{p}{D_p} + \frac{m}{D_m} \quad (1.1)$$

Db: overall body density, w: proportion of water, f: proportion of fat, p: proportion of protein, m: proportion of mineral, Dw: density of water, Df: density of fat, Dp: density of protein, Dm: density of mineral

Bio-electrical impedance (BIA) is used to measure volume, shape, or tissue electrical properties using a general formula [9]:

$$Z = \frac{\rho L}{A} \quad (1.2)$$

ρ is the resistance which is a metric of the tissue. L is the distance between the electrodes placed on the body. A is the area. Z is the impedance. By placing an electrode on the person's right hand and foot and sending a current through the body one measures the voltage and current with respect to time on each electrode and can determine body water and subsequently body fat. Fat and bone have higher resistance than fluid and electrolytes and thus the electrons travel differently through these mediums. Examples of great literature can be found in table 1.1.

Table 1.1: A normal size table. There has been a complaint that table captions are not single-spaced, but they should be. This is a test of that feature.

Title	Author
War And Peace	Leo Tolstoy
The Great Gatsby	F. Scott Fitzgerald

CHAPTER 2

PREVIOUS WORK

Previous work on this included a variety of 3d scanning machines.

Figure 2.1: Fit3d scanner



2.1 3d optical scanners

These scanners are all good and use a variety of kinect sensors and intel sensors. They are good but rather inflexible in serving the purpose of imaging in space. As such, I built my own system

for this. The software for these systems is not open source and depends heavily on the precise geometry of these systems

2.2 depth imaging

Next I review one of the most fundamental work on 3d imaging [8]. KinectFusion: Real-Time Dense Surface Mapping and Tracking was a seminal work in which Microsoft developed a time of flight sensor and developed algorithms for real time reconstruction of a scene. Their method comprises of 4 main parts. Part 1 is the surface measurement, which includees the raw depth measurements along with a dense vertex map and normal pyramid map being generated. Part 2 is the sensor pose estimation which is done by predicting the what the surface should be like from the previous data and using multi-scale iterative closest points to the current data. Part 3 is updating the reconstruction by fusing the current measurement with the scene model which is maintained with a truncated signed distance function. The final part is predicting the surface from part 3 which feeds back into part 2.

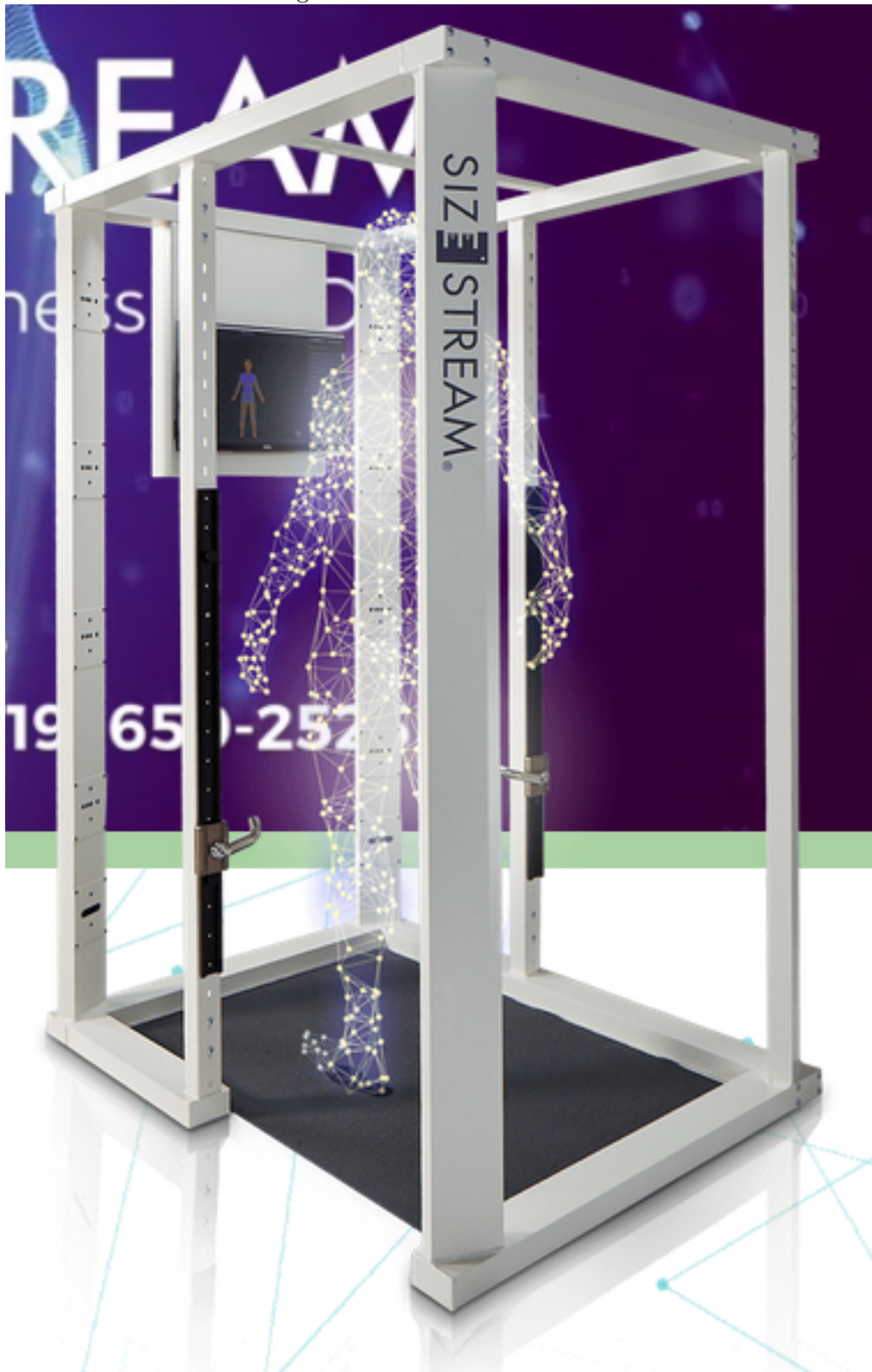
Figure 2.2: Naked Labs Scanner



Figure 2.3: Styku scanner



Figure 2.4: Sizestream scanner



CHAPTER 3

METHODS

There were several things I worked on. The first is a review of different sensor technologies and subsequent testing of the top ones. Next was the development for the Zero G Parabolic Flight which are scheduled for the summer. Third was simulating microgravity and testing them. Fourth was seeing the impact of pose on the resulting steps and final measurements.

I did a review of the sensor technologies out there excluding the commercial systems mentioned in previous works. I looked up their specs such as resolution, depth accuracy, and frame rate. I then benchmarked them on depth accuracy, temporal noise, spatial noise, and fill rate. These benchmarks were also done at varying distances. To do so, I made a simple setup. I used an imaging chart and a laser measure. I used 10 frames for each test. **The setup is shown here**

Machine Learning and Deep Learning work very well in many domains.

3.1 Graph Neural Network

One such deep learning method that is used for 3d data inputs are graph neural networks. The one I used specifically is called dynamic graph convolutional neural network (dgcnn). It consists of n vertices, each of which are tuple of 3 numbers. In order to apply the convolution operator, one must define an edge. With 2d images, an edge is any pixel that is adjacent to another pixel within the kernel length. For a graph, different distance metrics can be used. Dgcnn uses pairwise euclidean distances. The k nearest points are used for the subsequent convolution. Next comes the convolution kernel, which the authors define as

$$E_{ij} = ReLU(\theta_i * (x_j - x_i) + \theta_j * x_i) \quad (3.1)$$

Then comes max pooling for all such node j in the neighboring set of node i :

$$F_{ij} = Max(E_{ij}) \quad (3.2)$$

Before the point cloud goes into this architecture, they apply a matrix transformation using the coordinates and the differences with their neighbors. They prove certain desirable properties such as permutation invariance and translation invariance. And achieve state of the art results on classification and segmentation in June 2019. While they used their architecture for classification and segmentation, I convert it into regression for use in an automated caesar point placement. In Caesar, 75 landmarks are manually picked which allows a standardized template of 60k nodes to fit to the original mesh that has several hundred thousand points. Usually this takes several minutes for an expert user and can take up to an hour for a beginner. A landmark is defined as an $(x,$

y, z) coordinate and there are 225 such numbers that are needed to be predicted in a regression case. The other method is segmentation, which is reduced to classification of each point. In which there will be several hundred thousand points which will each need to be classified into 75 classes. Resulting in many predictions and some of these predictions may not even be exactly precise as the landmarks may not coincide directly with a point. It is hypothesized that training maybe easier in the beginning; however, in the long term one would expect a degradation in results because there is much noise. This noise comes from the fact that many points don't belong, and only 75 are really needed. With regression, one can predict the exact point and get to perfect performance. But the beginning of training may be more difficult as the predictions are totally random and the errors will be large.

3.2 Sensor Comparison

In order to choose the best sensor one could use intermediate metrics that define how good that sensor or one could use all of those sensors in the overall imaging setup and analysis and see which one works the best. Ideally, both should be done. I started with the first. The metrics thus defined are Z-accuracy, Fill Rate, spatial noise, and temporal noise. The Z-accuracy says how accurate the depth sensor is in relation to a ground truth(GT). We average the differences in depth sensor value and ground truth. Each metric is for a given single frame and was then average across 10 frames.

$$z - accuracy = \frac{1}{n} \sum_p (Image - GT) \forall p \in box \quad (3.3)$$

The fill rate relates to how many of the depth pixels are valid. This is useful as some sensors have high accuracy but low fill rate. This is the percentage of pixels that are non-zero.

$$Fill - rate = \frac{\sum_p [I_p >= 0]}{|p|} \forall p \in box \quad (3.4)$$

Spatial noise I define as the standard deviation divided by the mean distance. The RMS error or spatial noise is useful to determine the x-y noise from a plane that is approximately equidistant from the imaging sensor.

$$noise = \sqrt{\frac{1}{n-1} \sum_p (I_p - \bar{I}_p)^2} \forall p \in box \quad (3.5)$$

Last comes the temporal noise. Which is essentially the same as spatial noise except we take it across frames of the same pixel location.

$$temporal - noise = \sum_p \sqrt{\frac{1}{n-1} \sum_{f=1}^{10} (I_{pf} - \bar{I}_p)^2} \forall p \in box \quad (3.6)$$

These 4 metrics are what I test. In addition to that, I compare things such as frame rate, field of view, weight, dimensions, resolution, sdks, minimum z distance and maximum z distance.

3.3 Categorical Extreme Gradient Boosting

I used Catboost in order to model body composition using only demographic information and was able to achieve very good performance even better than previously published [referenced](#).

3.4 Parabolic Flight Setup

The original plan was to have parabolic flights during the summer of 2020 but when we started looking into dates for zero g flights, they had regular flights then but only had research flights during the spring and fall. Thus we chose to attempt to get ready for the spring. It was a bit rushed and we almost made it, ultimately though, zero g was not able to work through some deals with other companies and coronavirus also started ramping up at that time, so the flight was postponed. To take a 3d imaging system aboard such a flight required certain things that other people have not taken into consideration before when imaging humans for body composition. Some systems like the naked labs scanner have a mirror which encases the sensors. This is not necessary in zero g as one does not want any object to crack the mirror and the mirror is not needed for imaging. Other scanners such as the sizestream are extremely heavy and bulky and use many sensors. The height of this is larger than 60 inches which is the maximum height an object can be when brought onto the zero g flights. Thus I built my own imaging system. After testing the sensors, I selected the best one. Then tested different imaging parameters for the software such as frame rate, distance from the sensor, etc.

3.5 Creating the ideal imaging setup on plane vs on ground

There are a few differences with the ideal imaging setup on plane vs on ground. One such being timing. As each parabolic arc is limited to only 8-15 seconds of microgravity. So we only could shoot for 8 seconds at max to be safe. While on the ground, time is only a concern due to funding for the subject's time and their availability. Thus when choosing the best parameters on ground. I tested various setups. This included sensor type, frame rate, sensor height, rotation speed, laser power, minimizing laser interference. All included in the table [below](#).

3.6 body imaging on babies

Body imaging on babies is difficult because babies have trouble standing on their own. So typically they are imaged lying down. A result of this is the backside can not get imaged. The method we

tried using to get a mesh of babies was [smil](#). After getting it set up we got some preliminary results on fake babies that looked good. The original plan was to see how this could be used for this project too. As there are some cases where the entire body may not be able to be imaged. This includes on an inversion table where the back is once again obscured from view of the sensors regardless of positioning. Another is the timing issue on the parabolic flights in which one could stitch together an incomplete view of the person if needed.

3.7 3d mesh modeling of humans

A few methods were tried out such as recent deep learning methods [that take in an rgb image and produce a mesh](#). Also the classic kinect fusion code was tried out [paper](#). Finally a high level library of the kinect fusion code was used [recfusion](#).

3.8 microgravity simulation

Some other ways besides parabolic flight testing to simulate microgravity include gravity boots, inversion tables, and underwater imaging. The protocols were developed for these but scanning of participants was halted due to coronavirus.

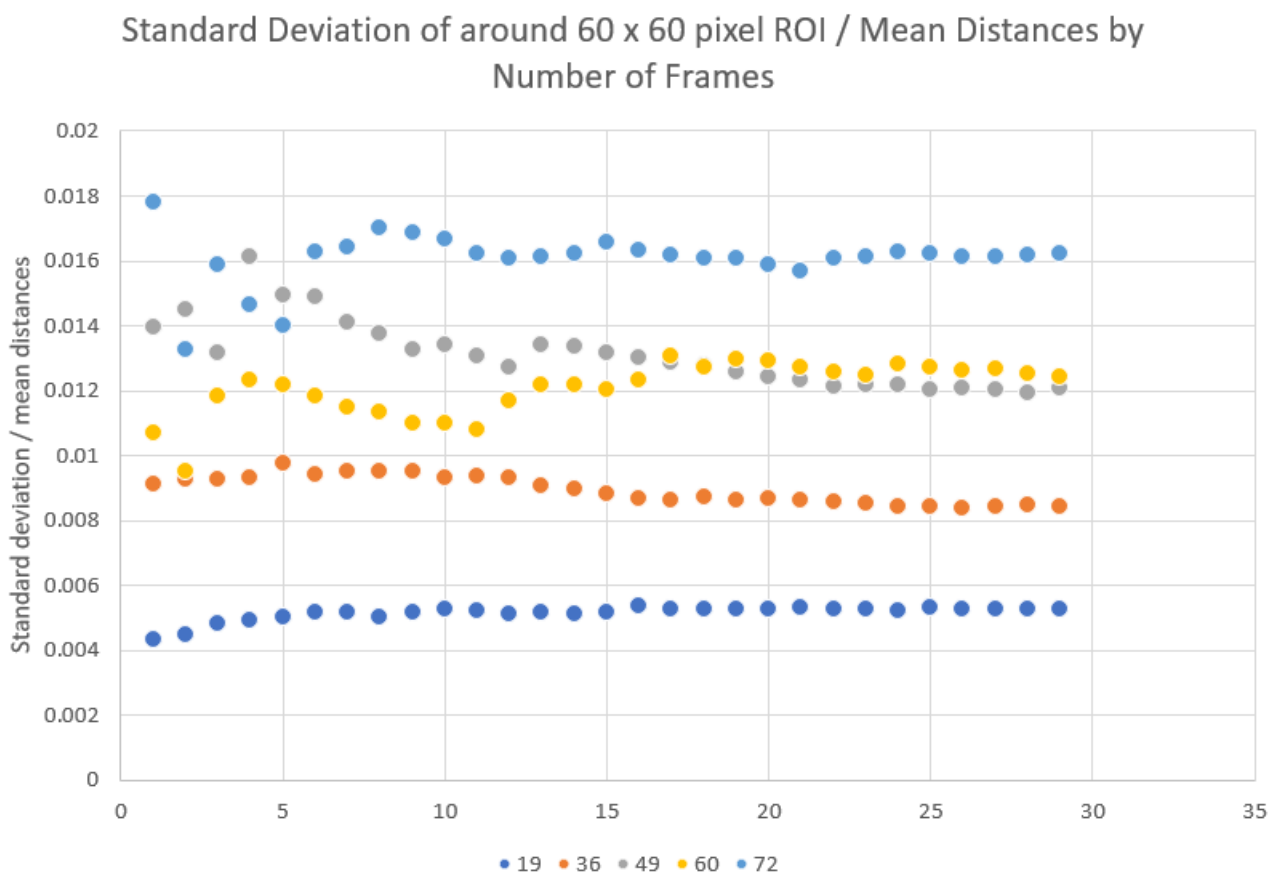
CHAPTER 4

RESULTS

4.1 sensor testing results

The below figure shows the spatial resolution per frame of the d435. This was done to test if the spatial noise changes with the number of frames and the distance. The number of frames does not appear to have an impact; however, the spatial noise is increasing relative to the distance.

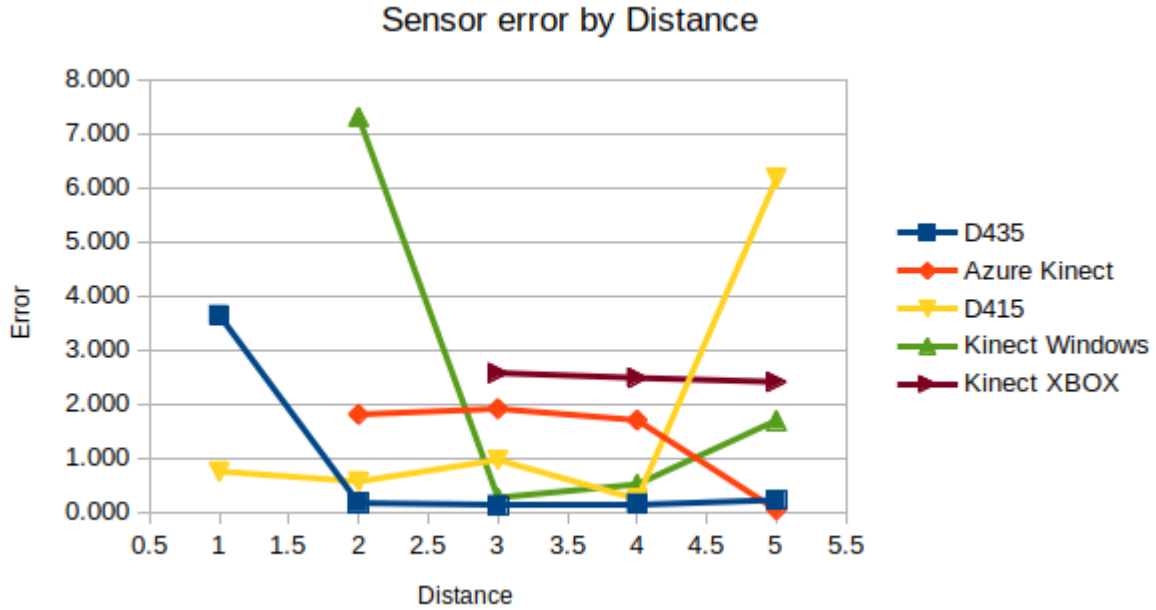
Figure 4.1: Spatial resolution per frame of d435



Here is the chart for sensor accuracy. The average errors by sensor are: 0.864 for the D435, 1.366 for the Azure Kinect, 1.739 for the D415, 2.446 for the Kinect Windows, and 2.489 for the Kinect XBOX.

Here is the chart for temporal noise. Whereas the D435 scored the best, the D415 scored the best in this category. This is partly explained by the d435 being like the d415 except having its

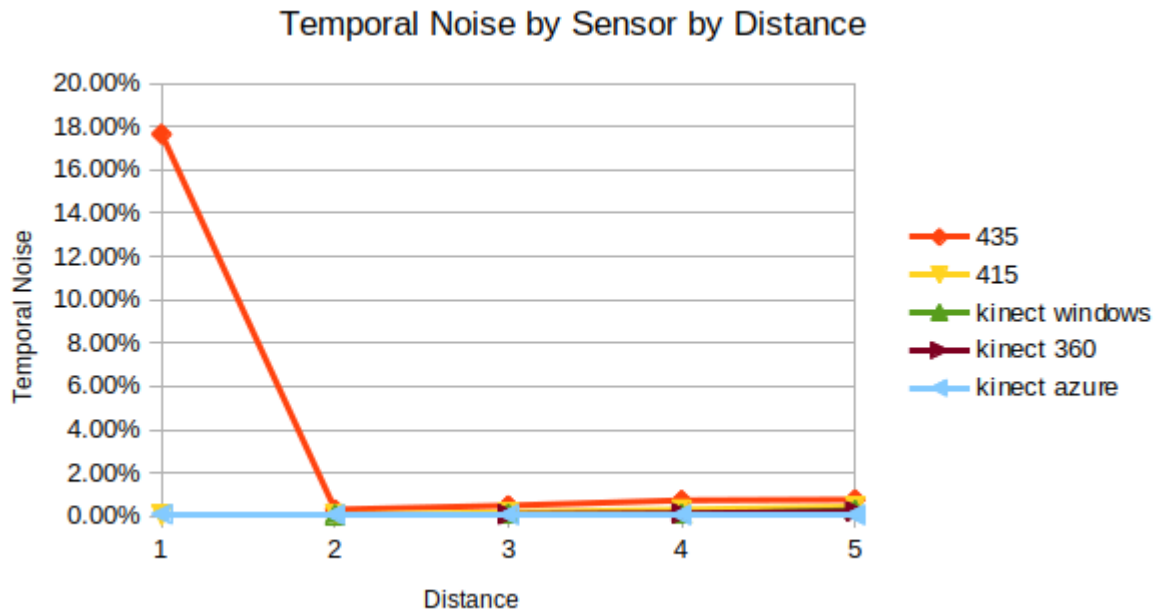
Figure 4.2: Sensor accuracy by distance



sensors more spread out. The winner in this category is the Kinect Azure with an average temporal noise of 0.07 percent, then comes the kinect for windows at 0.14, kinect 360 at 0.15, d415 at 0.22, and d435 and 3.99.

Here is the chart for fill rate. At first this metric may not seem that important but once you look at the actual depth images you can really see the difference between the sensors. If we exclude the kinect windows because it can't take data at 1 feet away and the kinect 360 which can't take data closer than 2 feet. The best sensors are d435 at 89.86 percent, d415 at 74.81, then Azure at 70.00. The Azure Kinect makes a very interesting design choice as the developers only keep pixels that the sensor is very confident in to maintain better accuracy. While the Kinect Windows and Kinect 360 trade this off by showing more valid pixels but have a reduced accuracy. With this judgement, it is even unclear whether the Azure kinect is even a better sensor in terms of specs as if one applied this same reduction in uncertain pixels in the kinect windows and kinect 360, those sensors may achieve comparable results.

Figure 4.3: Sensor temporal noise by distance



4.2 automated anthropometry results

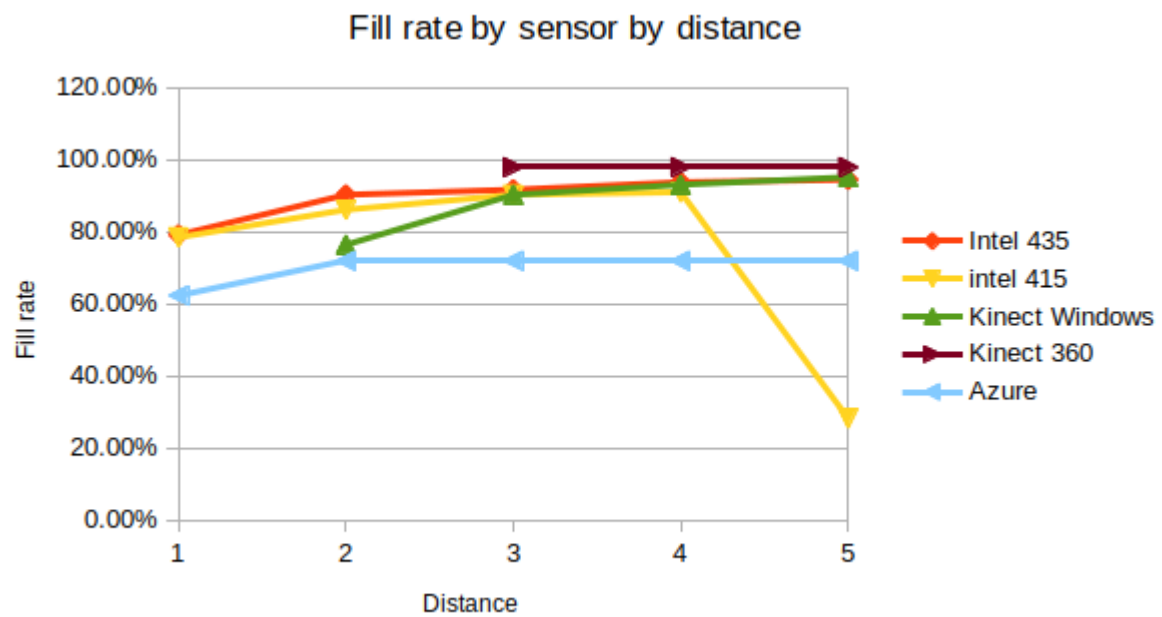
4.3 gradient boosting body composition results

4.4 graph neural network body composition results

4.5 3d imaging testing results

Results were as follows and are provided in the figures .

Figure 4.4: Fill rate of sensor by distance



CHAPTER 5

CONCLUSION

This is going to be the chapter where I check the length of the page to make sure the bottom margin works out all right. I hope you don't mind long annoying and useless paragraphs because you are sure to get a lot of them here!

5.1 Widgets

This is going to be the chapter where I check the length of the page to make sure the bottom margin works out all right. I hope you don't mind long annoying and useless paragraphs because you are sure to get a lot of them here!

5.1.1 Sub-Widgets

This is going to be the chapter where I check the length of the page to make sure the bottom margin works out all right. I hope you don't mind long annoying and useless paragraphs because you are sure to get a lot of them here!

Sub-Sub-Widgets

This is going to be the chapter where I check the length of the page to make sure the bottom margin works out all right. I hope you don't mind long annoying and useless paragraphs because you are sure to get a lot of them here!

Para-Widgets This is going to be the chapter where I check the length of the page to make sure the bottom margin works out all right. I hope you don't mind long annoying and useless paragraphs because you are sure to get a lot of them here!

Sub-Para-Widgets This is going to be the chapter where I check the length of the page to make sure the bottom margin works out all right. I hope you don't mind long annoying and useless paragraphs because you are sure to get a lot of them here!

This is going to be the chapter where I check the length of the page to make sure the bottom margin works out all right. I hope you don't mind long annoying and useless paragraphs because you are sure to get a lot of them here!

This is going to be the chapter where I check the length of the page to make sure the bottom margin works out all right. I hope you don't mind long annoying and useless paragraphs because you are sure to get a lot of them here!

margin works out all right. I hope you don't mind long annoying and useless paragraphs because you are sure to get a lot of them here!

APPENDIX A

SOME ANCILLARY STUFF

Ancillary material should be put in appendices, which appear before the bibliography.

APPENDIX B

MORE ANCILLARY STUFF

Subsequent chapters are labeled with letters of the alphabet.

BIBLIOGRAPHY

- [1] Carlina V Albanese, Evelyn Diessel, and Harry K Genant. Clinical applications of body composition measurements using dxa. *Journal of Clinical Densitometry*, 6(2):75–85, 2003.
- [2] Jacques Désarménien. How to run T_EX in french. Technical Report SATN-CS-1013, Computer Science Department, Stanford University, Stanford, California, August 1984.
- [3] Faq-O-Matic web site. <<http://www.dartmouth.edu/~jonh/ff-cache/1.html>>.
- [4] David Fuchs. The format of T_EX’s DVI files version 1. *TUGboat*, 2(2):12–16, July 1981.
- [5] David Fuchs. Device independent file format. *TUGboat*, 3(2):14–19, October 1982.
- [6] NJ Fuller, SA Jebb, MA Laskey, WA Coward, and M Elia. Four-component model for the assessment of body composition in humans: comparison with alternative methods, and evaluation of the density and hydration of fat-free mass. *Clinical Science*, 82(6):687–693, 1992.
- [7] Richard K. Furuta and Pierre A. MacKay. Two T_EX implementations for the IBM PC. *Dr. Dobb’s Journal*, 10(9):80–91, September 1985.
- [8] Shahram Izadi, David Kim, Otmar Hilliges, David Molyneaux, Richard Newcombe, Pushmeet Kohli, Jamie Shotton, Steve Hodges, Dustin Freeman, Andrew Davison, et al. Kinectfusion: real-time 3d reconstruction and interaction using a moving depth camera. In *Proceedings of the 24th annual ACM symposium on User interface software and technology*, pages 559–568, 2011.
- [9] Michel Y Jaffrin and Hélène Morel. Body fluid volumes measurements by impedance: A review of bioimpedance spectroscopy (bis) and bioimpedance analysis (bia) methods. *Medical engineering & physics*, 30(10):1257–1269, 2008.
- [10] Donald E. Knuth. The WEB system for structured documentation, version 2.3. Technical Report STAN-CS-83-980, Computer Science Department, Stanford University, Stanford, California, September 1983.
- [11] Donald E. Knuth. *The T_EX Book*. Addison-Wesley, Reading, Massachusetts, 1984. Reprinted as Vol. A of *Computers & Typesetting*, 1986.
- [12] Donald E. Knuth. Literate programming. *The Computer Journal*, 27(2):97–111, May 1984.
- [13] Donald E. Knuth. A torture test for T_EX, version 1.3. Technical Report STAN-CS-84-1027, Computer Science Department, Stanford University, Stanford, California, November 1984.

- [14] Donald E. Knuth. *T_EX: The Program*, volume B of *Computers & Typesetting*. Addison-Wesley, Reading, Massachusetts, 1986.
- [15] Leslie Lamport. *L^AT_EX: A Document Preparation System. User's Guide and Reference Manual*. Addison-Wesley, Reading, Massachusetts, 1986.
- [16] Oren Patashnik. *BibT_EXing*. Computer Science Department, Stanford University, Stanford, California, January 1988. Available in the BibT_EX release.
- [17] Oren Patashnik. *Designing BibT_EX Styles*. Computer Science Department, Stanford University, January 1988.
- [18] Arthur L. Samuel. First grade T_EX: A beginner's T_EX manual. Technical Report SATN-CS-83-985, Computer Science Department, Stanford University, Stanford, California, November 1983.
- [19] Michael D. Spivak. *The Joy of T_EX*. American Mathematical Society, 1985.